Velocity measurement inside a diesel spray by using time-resolved PIV under high ambient density condition

Y. Zama*, W. Ochiai, T. Furuhata and M. Arai
Department of Mechanical System Enginering, Gunma University
1-5-1, Tenjin-cho, Kiryu, 376-8515, Japan
yzama@gunma-u.ac.jp, t11801209@gunma-u.ac.jp,
tfuruhata@gunma-u.ac.jp and arai@gunma-u.ac.jp

Abstract

In a direct injection diesel engine, its boost pressure tends to increase for improvement of engine performance. High boost pressure resulted in an increase of gas density in engine cylinder, and the high gas density affected the diesel spray behavior and mixture formation of fuel and air. Therefore, under high gas density condition, precise investigation of spray behavior was required. In this paper, in order to understand spray behavior in high gas density surroundings, velocity field inside a diesel spray was measured with time-resolved particle image velocimetry (PIV). Velocity distributions were investigated with various ambient gas densities and injection pressures. As the results, in high gas density surroundings, cluster of spray droplets near the spray periphery hardly moved, and it was re-entrained into main spray flow. These phenomena were coupled with vortex formation near the spray periphery. Moreover, from normalized axial velocity distribution, it was clear that the position of intense mixing zone at Z = 40mm shifted from the periphery to the inside of spray with increasing ambient gas density and injection pressure. However, its trend did not appear for normalized axial velocity distribution at Z=60mm.

Introduction

Recently, exhaust gas recirculation (EGR) ratio and boost pressure of a diesel engine tend to increase for improvement of diesel engine performance and emission. In ultra-high boost engine, compressed gas density in combustion chamber became 3 or 4 times higher than that in natural aspirated (NA) engine [1]. It seems that a diesel spray behavior in high gas density surroundings might differ from that in a conventional diesel engine. There are many reports regarding the effect of ambient gas density on diesel spray behavior. Roisman et al.[2] investigated the relationship between ambient gas density and spray tip penetration. However, their results were limited within the range of ambient gas density similar to NA diesel engine condition. Klein-Douwel et al. [3] reported the spray tip penetration and spray angle under ambient gas density that was 3 times higher than the conventional diesel engine. Effect of ambient gas density on spray angle was also investigated by Delacourt et al.[4] and Sovani et al.[5]. They evaluated the spray angle in high gas density surrounding similar to an ultra-high boost engine condition.

Regarding the investigation of spray behavior and spray velocity, there were some results obtained with Laser Doppler Velocimetry (LDV) and Particle Image Velocimetry (PIV). PIV is velocity field measurement technique with high spatial resolution and is currently applied to various sprays. There are some PIV reports regarding velocity of air entrainment motion around diesel spray [6][7][8][9]. However, a few investigations on the velocity measurement inside of diesel spray were carried out. Cao et al.[10] evaluated velocity field inside the spray by using PIV combined with laser induced fluorescence (LIF) technique. They obtained successfully the velocity distribution inside the spray, and discussed a vortex structure in the spray. However, they only obtained single instantaneous velocity field inside the spray because of a performance limitation of the conventional PIV system. To understand the diesel spray behavior completely, both of instantaneous and time averaged velocity fields need to be investigated. Especially, temporal change of velocity field inside the spray should be investigated in order to understand the mechanism of the mixture formation between the spray and the surrounding air. Therefore, it is necessary to obtain not only instantaneous velocity field but also temporal change of velocity fields for the analysis of transient and average behavior of diesel spray.

Recently, high speed camera with high spatial resolution has been developed and commercialized. As the result, Hayami et al.[11] developed time-resolved PIV system called Dynamic PIV to obtain velocity field with high spatial and high temporal resolution. It consisted of high speed camera and high repetition double-pulsed Nd:YLF laser. They successfully obtained time-series velocity fields of water-spray jet with temporal resolution of 10kHz. Thus time-resolved PIV becomes a promising technique for velocity measurement of high-

* Corresponding author: yzama@gunma-u.ac.jp

speed and unsteady flow. An advantage of this technique for diesel spray application is that many instantaneous velocity fields could be reconstructed from sequential spray images over 100kHz. Thus it is easy to evaluate ensemble mean velocity field from sequential velocity fields of a single shot diesel spray. Authors [12] applied the time-resolved PIV to a measurement of velocity field inside a diesel spray. As the results, radial *mean* velocity distribution of diesel spray was obtained and intense mixing zone was discussed using the gradient of velocity distribution. However, effects of injection pressure and surrounding gas density on intense mixing zone were hard to discuss because of limited experimental data.

In this study, velocity distribution inside diesel spray was measured in various gas density surroundings and injection pressures. Maximum velocity gradient positions were evaluated using the Gaussian type distribution function fitted to velocity distribution. Further, effects of ambient gas density and injection pressure on these positions were discussed.

Experimental setup

Figure 1 shows schematic view of experimental set-up. It consisted of a fuel injection system, a high pressure vessel and an optical system for visualization of a diesel spray. The high pressure vessel was filled with N_2 gas. The diameter of injection nozzle hole was 0.17mm. Test fuel was JIS No.2 diesel fuel. Using a single-hole diesel nozzle with a single shot injection system, diesel fuel was injected into the pressure vessel. Sequential shadow images of the spray were captured with a high-speed camera (Photoron, PCI-512). It was applied to measure a spray width.

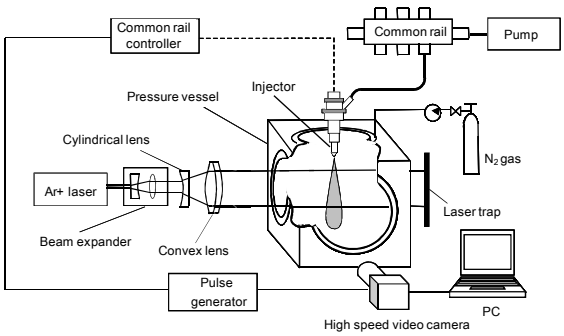

Fig.1 Experimental set-up (PIV)

For velocity measurement inside a diesel spray, Ar^+ ion continuous laser was utilized as a light source, and a laser-light sheet was formed. Then a tomographic image of a diesel spray was obtained. The thickness of laser-light sheet was adjusted and set on 1mm to obtain high quality images for PIV analysis. Digital high-speed camera (Vision Research, Phantom V710) was arranged in perpendicular position to the laser-light sheet, and sequential images of a diesel spray were captured. Center position of observation area was set on Z = 40mm or 60mm from a nozzle.

Table 1 Experimental conditions

Injector type	Single hole			
Nozzle hole diameter [mm]	0.17			
Test fuel	Diesel fuel (JIS No.2)			
Ambient temperature [K]	300			
Ambient pressure P_a [MPa]	0.5	1.0	2.0	4.0
Ambient density ρ_a [kg/m^3]	5.8	11.6	23.2	46.5
Injection period t_{inj} [ms]	3.2			
Injection pressure P_{inj} [MPa]	60	90	120	150
Injection mass M_{inj} [mg]	21.6	25	28.5	31.5

Experimental conditions are shown in Table 1. Ambient gas temperature in the high-pressure vessel was 300K, and then ambient gas density ρ_a was set on from 5.8kg/m^3 to 46.5kg/m^3 under the room temperature condition. Here, ambient gas density of 11.6kg/m^3 at P_a = 1.0MPa was equivalent for a compressed air density of 3MPa at 800K. This pressure and temperature corresponded to a combustion chamber condition at injection timing of a conventional NA diesel engine. Injection period was set to 3.2ms. Moreover, various injection pressures were tested. Under the constant period injection, total injection mass of test fuel and injection rate changed with injection pressure. Since an effective injection pressure was slightly changed with surrounding pressure, the injection mass of fuel was not influenced with ambient gas density under the same injection pressure condition.

Effect of ambient gas density and injection pressure on diesel spray width

Using image processing method, spray width was obtained from sequential shadow images of diesel spray. The procedure for spray width analysis is shown in Fig. 2. The sequential shadow images of spray were captured from injection start to injection end. In order to obtain the mean shape of a spray, unsteady spray fluctuation should be eliminated, and sequential spray images only in the steady state period where injection rate fluctuation was small were averaged. Then spray width was obtained from the averaged shadow image using a threshold of photo-density. Here, 50% and 10% values of photo-density were selected as the threshold to distinguish the spray periphery

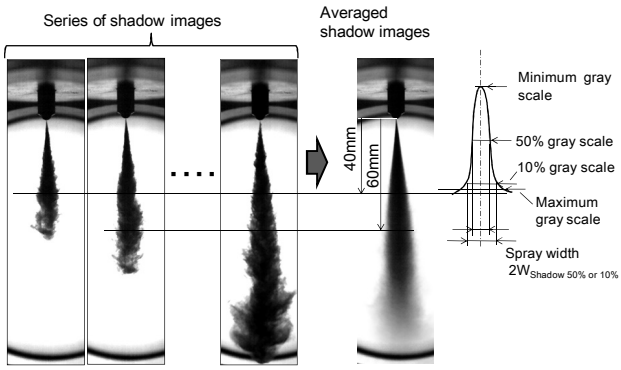

Fig. 2 Procedure of image processing for spray width analysis

from background image. Here, spray width obtained by 10% value seems like the conventional spray width obtained by classical photographic measurement and spray width by 50% seems like little narrower than that.

Figure 3 shows spray width $2W_{shadow\ 50\%}$ and $2W_{shadow\ 10\%}$ at Z = 40mm and 60mm for various ambient gas densities and injection pressure. $2W_{shadow\ 50\%}$ is shown as a solid line, and $2W_{shadow\ 10\%}$ is a dashed line. At Z = 40mm, spray width increased with an increase of ambient gas density. Moreover, the width slightly increased with an increase of injection pressure. Spray width change with ambient gas density was larger than that with injection pressure. Those trends did not depend on threshold definitions of spray boundary. At Z = 60mm, spray width increased also with an increase of ambient gas density and injection pressure.

By taking into physical meaning of spray width and spray angle, they have almost the same meaning. As for increasing trend of spray width with ambient gas density, it corresponded well to a trend of spray angle increase with ambient pressure [13]. Moreover, Wakuri et al.[14] reported that injection pressure effect on spray angle was small. Their suggestion corresponded well to the measured trend of spray width increase with injection pressure. Therefore, under high ambient gas density condition corresponding to ultra-high boost engine, ambient gas density and injection pressure effects on spray width were similar to these of previous literatures.

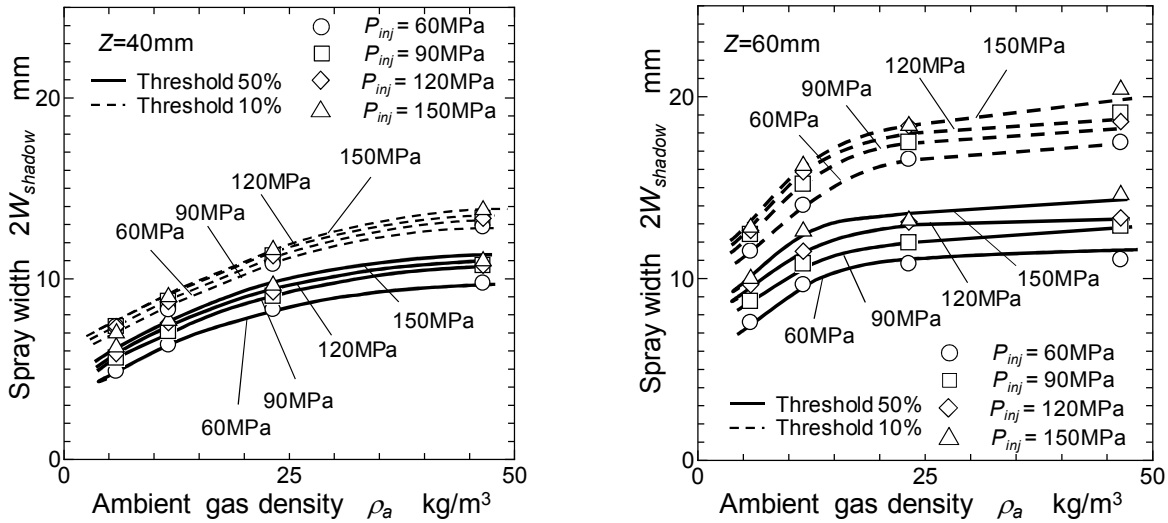

(a) Z = 40mm (b) Z = 60mm

Fig. 3 Spray width vs. ambient gas density

Time-resolved PIV measurement for velocity distribution inside diesel spray

Time-resolved PIV analysis was applied to measure velocity field inside a spray. For PIV analysis, correlative tomographic images with narrow time interval were required. Thus optimum frame rate of the digital high-speed camera was selected by considering spray velocity that depended on injection pressure and ambient gas density. Consequently, the frame rate was set to be a spray displacement around 5 pixels on sequential images. Since an ultra-high frame rate over 100,000 f.p.s was needed for PIV analysis, image size was restricted by the performance of digital high-speed camera. Thus image size and view area were changed with ambient gas density and injection pressure conditions. However, spatial resolution was fixed constant at 0.08mm/pixel regardless of injection pressure and ambient gas density.

According to the insufficient spatial resolution (0.08mm/pixel) of an image, each droplet in a spray could not be resolved on an image. Inside diesel spray, number density of the droplets was very high. Consequently, cluster of spray droplets could be captured as photo-density distribution in a spray image. Thus velocity distribution of droplet cluster could be obtained with PIV analysis based on direct cross-correlation method with sub-pixel accuracy. In general, for the unresolved particle image, accuracy of PIV measurement is degraded because a peak of the cross-correlation function is not clear. Therefore, in this PIV analysis, displacement error with sub-pixels might be included in the results of velocity distribution.

In this PIV analysis, interrogation spot size was 23pixels×23pixels which coincided with 1.84mm×1.84mm of real image, and interrogation spot area of 50% was overlapped with the adjacent interrogation area. It means that grid space in PIV analysis was 0.92mm. Regarding evaluation area for PIV analysis, droplet cluster of opposite to the laser incident side could not be imaged clearly due to light absorption with spray of laser incident side. Then the incident side area of spray image was focused for discussion of velocity distribution, though PIV analysis was carried out on a whole spray image.

Instantaneous velocity field inside diesel spray

Time-series of instantaneous velocity fields in a diesel spray are shown in Fig. 4. In these figures, analyzed area was located at around Z = 40mm. Vector maps were superposed on tomographic spray images processed in PIV analysis. τ means elapsed time from injection start. Figure 4 (a) and (b) show vector maps for different ambient gas densities at highest injection pressure among experimental conditions. Time-series velocity fields at another injection pressure are shown in Fig. 4 (c).

Figure 4 (a) shows the velocity field in the conditions of P_{inj} = 150MPa and ρ_a = 11.6kg/m^3 (Pa =1.0MPa). The spray tip moved to a direction of downstream. Spray tip velocities obtained at τ=0.280ms and 0.288ms were almost the same. As for a spray part following the tip, velocity fields are shown in vector maps of τ=0.631ms, 0.657ms and 0.680ms. In these maps, velocities near the periphery of spray decreased as compared with those near the spray center. It was caused by momentum exchange between ambient gas and spray droplets, even though spray periphery moved to a direction of spray penetration. Moreover, spray velocity of upstream part was larger than that of the downstream as shown in τ=0.657ms. It means that spray of the upstream part caught up the downstream part.

In high gas density surroundings condition shown in Fig. 4 (b) (P_{inj} = 150MPa and ρ_a = 46.5kg/m^3), according to the velocity maps and photo-density distributions at τ = 0.684ms and 0.770ms, spray tip looked like expanding with elapsed time. Photo density around a spray tip decreased with elapsed time. Thus it could be considered that dispersion of a spray (droplets cluster) around the tip progressed with elapsed time. When velocity fields at τ = 0.770 and 2.615ms were focused on, a part of droplet cluster moved to radial direction by spray fluctuation. At τ = 0.864 and 2.768ms, velocity of the cluster near the spray periphery decreased due to momentum exchange between spray droplets and ambient gas. Thus the cluster hardly moved near the spray

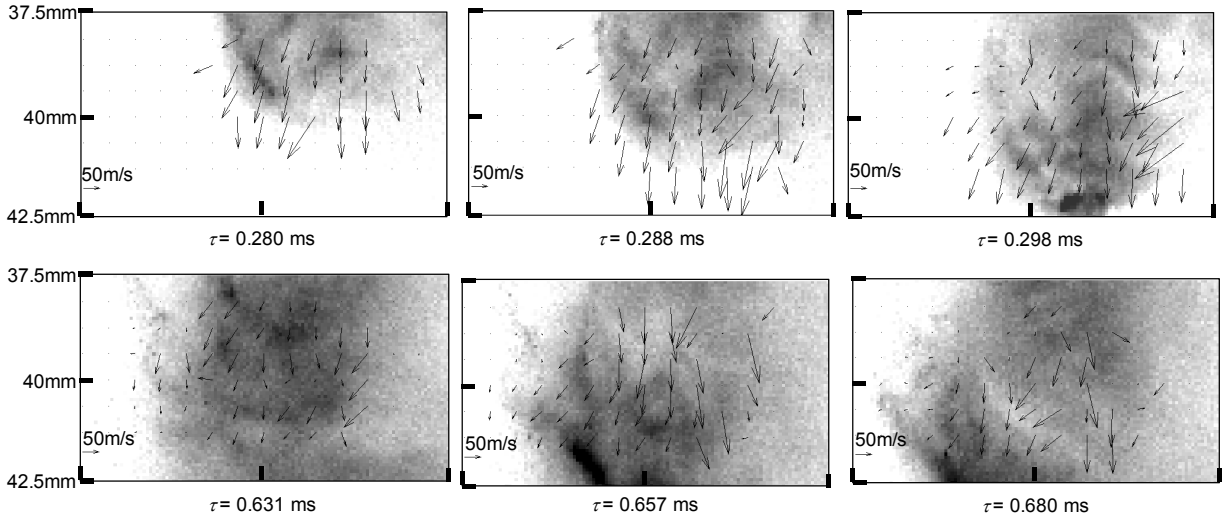

(a) P_{inj} = 150MPa and ρ_a = 11.6kg/m^3

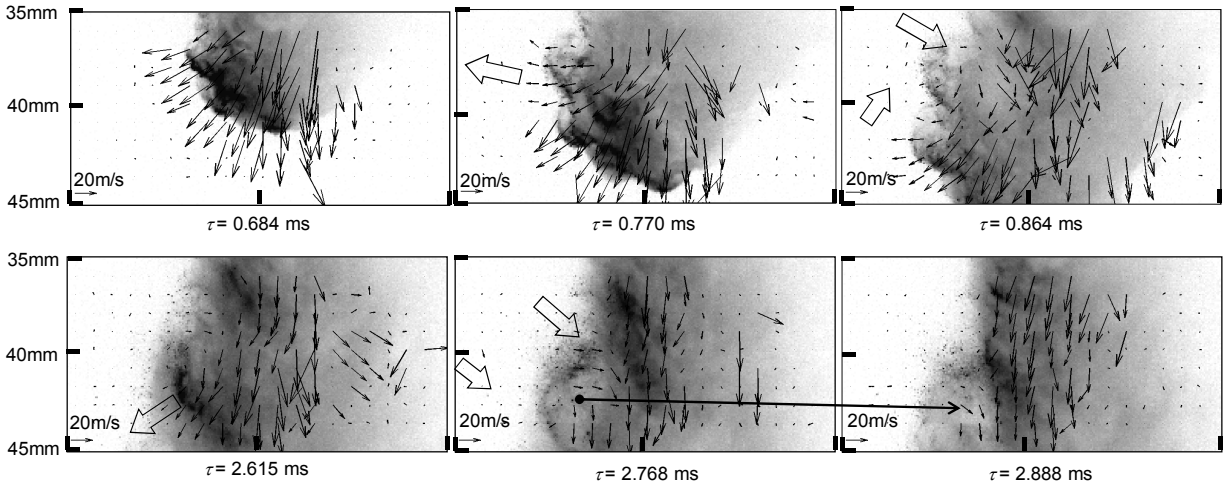

(b) P_{inj} = 150MPa and ρ_a = 46.5kg/m^3

Fig. 4 Instantaneous velocity fields inside diesel spray

(Continued to next page)

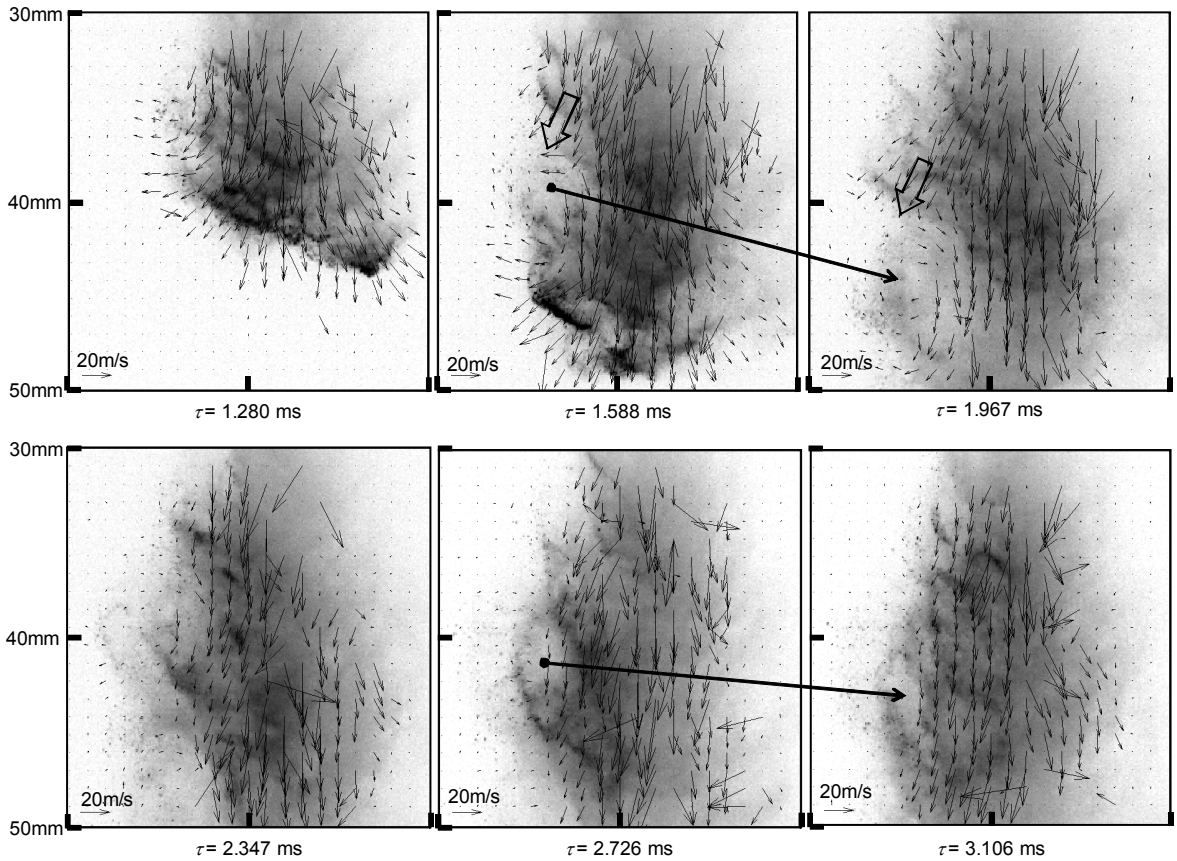

(c) P_{inj} = 60MPa and ρ_a = 46.5kg/m^3

Fig. 4 Instantaneous velocity fields inside diesel spray

periphery, and a part of cluster droplets near the periphery was re-entrained into the main stream of the spray. Finally, a vortex near the spray periphery was formed. At τ = 2.768ms and 3.106ms, the spray cluster near the periphery was stagnated at almost the same position, and density of droplet cluster decreased due to a re-entrainment of lean droplet cluster into the main stream.

By increasing ambient gas density, spray velocity decreased dramatically. For example, velocity near spray center at 11.6kg/m^3 (Fig. 4(a)) was around 100m/s, and the velocity at 46.5kg/m^3 (Fig. 4(b)) was around 50m/s. Therefore, it seems that momentum of spray droplets was consumed by entrainment of high gas density surroundings. Moreover, a vortex appeared clearly near the spray periphery in high ambient gas density surroundings. It seems that velocity difference between main stream and the periphery became large by an increase of ambient gas density.

Figure 4(c) shows vector maps of the spray injected by low injection pressure (P_{inj} = 60MPa) into high gas density surroundings (ρ_a = 46.5kg/m^3). Velocities at the spray tip were slower than that just inside the tip. Zhu et al.[15] investigated velocity field of surrounding gas of a diesel spray using LIF-PIV technique. They clarified that the surrounding gas was pushed by the spray tip to a direction of spray development. By taking into their result, it seems that spray tip velocity that was slower than just inside velocity, was caused by momentum exchange between the spray and surrounding gas. It means that the momentum exchange corresponded to a driving force of surrounding gas movement. At the spray periphery, a vortex was formed with re-entrainment of lean surrounding spray cluster. When τ = 1.588ms and 1.967ms were focused on, this vortex moved to a direction of spray penetration. Spray clusters with high velocities appeared at upper side of the vortex. Then the vortex was pushed to the downstream direction with this cluster and was accelerated. However, during τ = 2.726ms to 3.106ms, another vortex appeared, but it slightly moved to the downstream direction.

By decreasing injection pressure, injection mass rate decreased, and also momentum of spray decreased. Spray tip movement at low momentum condition was weaker than that at high momentum condition. Thus pushing motion of spray tip appeared clearer than that of high momentum condition. Moreover, vortex size of lower momentum condition was larger than that of higher momentum condition. However, mechanism of vortex formation did not differ between these conditions. Finally, in high gas density surroundings, a vortex was formed clearly near the spray periphery, and ambient gas and spray droplets were re-entrained into main stream

of the spray. It seems that local mixture formation of spray and surrounding gas was caused by vortex formation near the periphery.

Mean velocity distribution inside diesel spray and intense mixing zone

In order to evaluate ensemble mean axial velocity distribution, instantaneous velocities analyzed with PIV were averaged in steady state period of injection. Moreover, three averaged velocity distributions obtained from the same injection condition were averaged again for each gas density condition. It means that over 1000 elemental PIV velocity distributions were averaged to obtain the mean velocity distribution of a given condition.

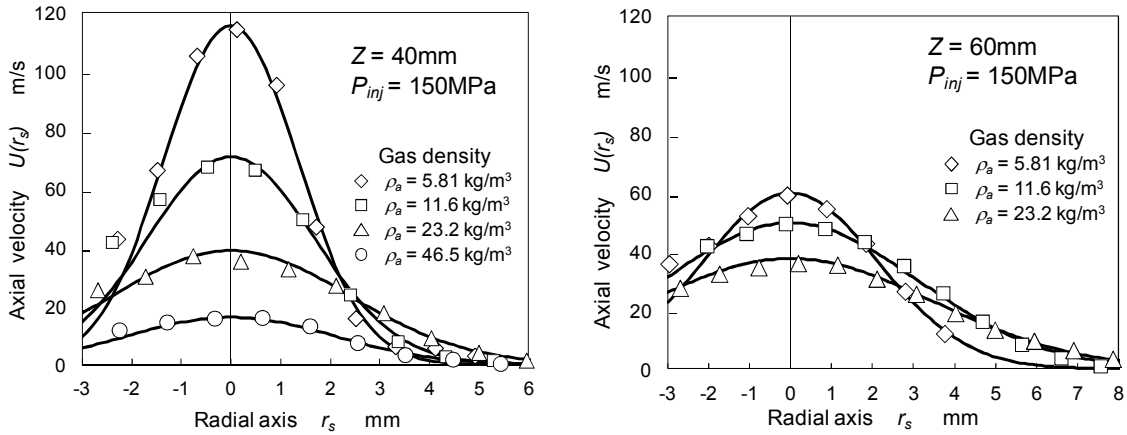

Fig. 5 Ensemble mean velocity distribution inside diesel spray

Figure 5 is radial distributions of mean axial velocity at 40mm and 60mm apart from nozzle exit. In the figure, experimental plots of various ambient gas densities at P_{inj} = 150MPa are shown. Velocity distribution at ρ_a = 46.5kg/m^3 at Z = 60mm could not be shown because data numbers of instantaneous velocity fields were not enough to obtain the ensemble mean velocity.

Zjinen et al.[16] used Gaussian type function for fitting analysis of velocity distribution of a single phase free jet. In this study, Gaussian function expressed with Eq. (1) was also introduced even though diesel spray was two phase flow of liquid and gas.

$$U(r_s) = U_c \exp\left(-\frac{r_s^2}{2\sigma^2}\right) \qquad (1)$$

Where, $U(r_s)$ is axial velocity of a spray, U_c is the maximum axial velocity, r_s is origin of radial axis (real center axis of spray), and σ is standard deviation of velocity distribution in Gaussian function. Appling least squares method to velocity distributions shown in Fig. 5, a set of U_c , σ, and r_s was fixed for each distribution of velocities.

Standard deviation σ was considered to be a characteristics index of radial dispersion of spray jet velocity. From Eq. (1), radial position where velocity gradient was maximum could be evaluated. Considering the physical meaning of maximum velocity gradient, its radial position seems to correspond with highest shear stress position, and also intense mixing zone might be formed around there. This position can be obtained with second order differential coefficient of Eq. (1) being set zero as shown in Eq. (2).

$$\frac{d^2}{dr_s^2}\left(\frac{U(r_s)}{U_c}\right) = 0 \qquad (2)$$

$$r_s = \sigma \qquad (3)$$

Then $r_s = \sigma$ shown in E.q. (3) was obtained. Thus normalized velocity at the maximum gradient location was 0.606 in Eq. (4) when r_s is set σ. It meant that intense mixing zone might appear at the radial distance $r_s = \sigma$, and velocity of this position was 60.6% of center velocity.

$$\left.\frac{U(r_s)}{U_c}\right|_{r_s=\sigma} = 0.606 \qquad (4)$$

Ambient gas density effect on the position of intense mixing zone, that is the effect on standard deviation, was evaluated. Figure 6 shows relationship between ambient gas density and standard deviation for various injection pressure conditions. Figure 6 (a) shows the relationship at Z = 40mm, and (b) is the one at Z =60mm.

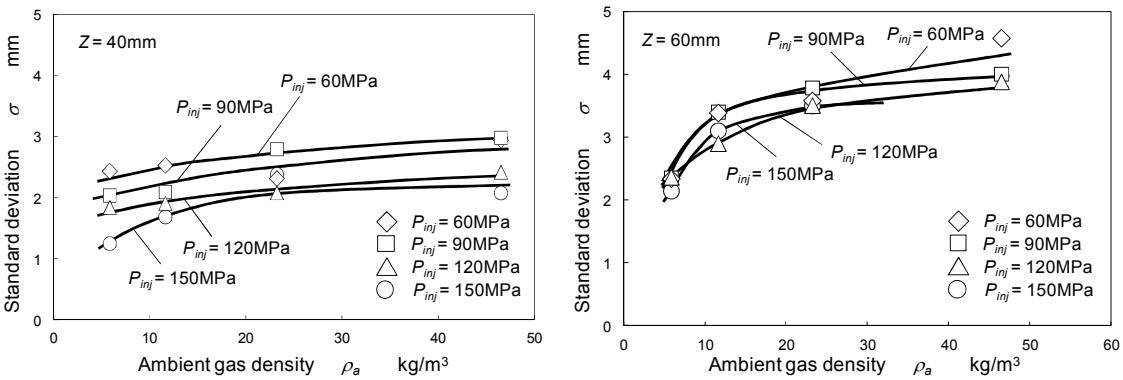

(a) Z = 40mm (b) Z =60mm

Fig. 6 Standard deviation of velocity distribution vs. Ambient gas density

Regardless of spray axial positions (Z axis) and injection pressures, standard deviation of velocity distribution increased with increasing the ambient gas density. At Z = 40mm, the standard deviation decreased with an increase of injection pressure. However, at Z = 60mm, the standard deviation difference by injection pressure became small as compared with that at Z = 40mm. According to E.q. (1), distribution of dimensionless spray velocity was determined with standard deviation. Therefore, it seems that radial distribution of axial velocity at Z =60mm had similarity regardless of injection pressures.

In order to understand a relative position of maximum velocity gradient in the spray, dimensionless position of maximum velocity gradient was evaluated as shown in Fig. 7. Vertical axis shows the relative position of maximum velocity gradient. It was calculated with standard deviation shown in Fig.6 and spray width of 50% threshold shown in Fig. 3.

In the case of Z = 40mm shown in Fig. 7 (a), the relative position of maximum velocity gradient was changed with ambient gas density. Under low injection pressure conditions, the relative position shifted from the spray periphery to inside of a spray with increasing ambient gas density. Moreover, the relative position

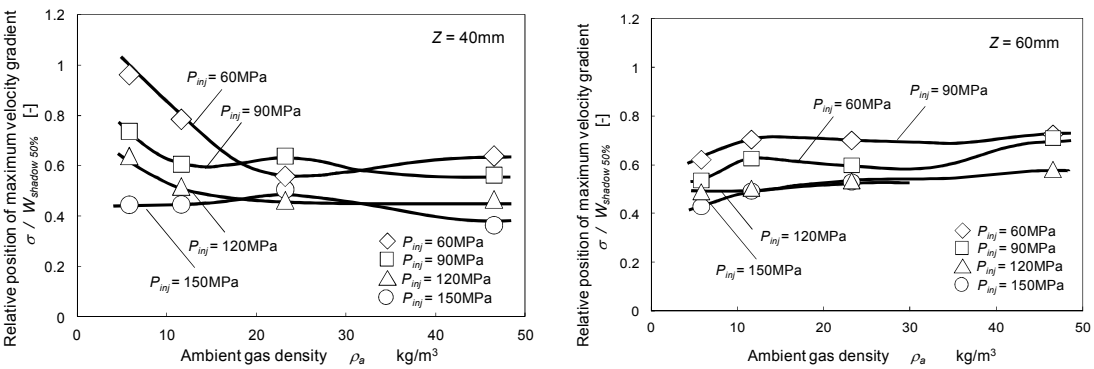

(a) Z = 40mm (b) Z =60mm

Fig. 7 Dimensionless position of maximum velocity gradient vs. ambient gas density (50% threshold)

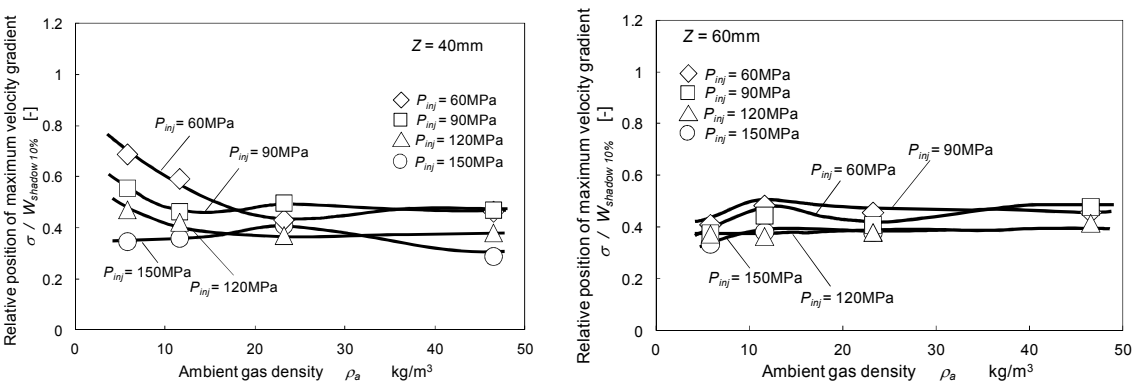

(a) Z = 40mm (b) Z =60mm

Fig. 8 Dimensionless position of maximum velocity gradient vs. ambient gas density (10% threshold)

was changed with injection pressure, and the position shifted from the periphery to spray inside with an increase of injection pressure. It means that position of intense mixing zone shifted from spray periphery to inside of a diesel spray with increase of ambient gas density and injection pressure. Therefore more internal mixing was promoted with increasing both of ambient gas density and injection pressure. On the other hand, at Z = 60mm shown in Fig. 7(b), as compared with Z = 40mm, the relative position change by ambient gas density was not clear. It seems that sprays at Z = 60mm was dominated with fully developed spray flow, and position shift by ambient gas density did not appear clearly.

The relative positions evaluated with spray width of 10% threshold are shown in Fig. 8. At Z = 40mm, although dimensionless value of the positions differed from those of 50% threshold, the position shifted from the periphery to spray inside with increasing ambient gas density and injection pressure. According to Fig. 3, spray width of 10% threshold was wider than that of 50% threshold, and the relative position evaluated with 10% threshold was more inside of the spray than that of 50% threshold. Spray boundary by 10% threshold might be recognized as conventional spray width in common sense. Therefore it means that intense mixing zone was formed inside the spray.

Conclusions

In this paper, diesel spray behavior under various ambient pressure and injection pressure condition was investigated with velocity distribution inside the spray by using time-resolved PIV. Insights of this study are as follows,

(1) Spray width of a diesel spray increased with increasing ambient gas density. On the other hand, the width slightly increased with increasing injection pressure.

(2) According to instantaneous velocity distribution in time series, near the spray periphery, there was a spray part that hardly moved to a direction of spray penetration. Then the spray part near the periphery was re-entrained into main spray flow. Finally, vortex flow was formed around spray periphery with elapsed time progressed.

(3) Velocity distribution of spray could be approximated with Gaussian type function as well as single phase free jet. Standard deviation σ of radial distribution of axial velocity, which was obtained by fitting of Gaussian function, increased with increasing ambient gas density. At Z = 40mm, it decreased with an increase of injection pressure, but this tendency became unclear at Z = 60mm.

(4) At Z = 40mm, the relative position of intense mixing zone shifted from spray periphery to spray inside with an increase of the ambient gas density and injection pressure. However, its trend did not appear clearly in normalized axial velocity distributions at Z = 60mm.

Acknowledgements

The digital high-speed camera used for PIV measurement was provided by Nobby Tech. Ltd. We would like to express special thanks to Nobby Tech. Ltd.

References

[1] Kobayashi, M., Aoyagi, Y., Adachi, T., Murayama, T., Noda, A., Goto, Y. and Suzuki, H., *COMODIA-200*8, Sapporo, Japan, July 28-31, 2008.
[2] Roisman, I., V., Araneo, L. and Tropea, C., *Int. J. Multiphase flow*, 33:904-920 (2007).
[3] Klein-Douwel, R.J.H., Frijters, P.J.M., Somers, L.M.T., de Boer, W.A. and Baert, R.S.G., *Fuel*, 86:1994-2007 (2007).
[4] Delacourt, E., Desmet, B. and Besson, B., *Fuel*, 84,859-867 (2005).
[5] Sovani, S. D., Chou, E., Sojka, P.E., Gore, J.P., Eckerle, W.A. and Crofts, J.D., *Fuel*, 80, 427-435 (2001).
[6] Driscoll, K. D., Sick, V. and Gray, C., *Exp. in Fluid*, 35, 112-115 (2003).
[7] Moon, S., Matsumoto, Y., Nishida, K. and Gao, J., *Fuel*, 89, 3287-3299 (2010).
[8] Sepret, V., Bazile, R., Marchal, M. and Couteau, G., *Exp. in Fluid*, 49, 1293-1305 (2010).
[9] Rajalingam, B. and Farrell, P., *SAE technical paper*, 1999-01-0523 (1999).
[10] Cao., Z., Nishino, K., Mizuno, S. and Torii, K., *Exp. in Fluid*, 29, S211-S219 (2000).
[11] Hayami, H., Okamoto, K., Aramaki, S. and Kobayashi, T., *5th Int. Symp. on PIV*, Busan, Korea, September 22-24, 2003.
[12] Zama, Y., Ochiai, W., Furuhata, T. and Arai, M., *15th annual conf. on liquid atomization and spray systems-Asia*, Pingtung, Taiwan, Oct 20-21, 2011.
[13] Hiroyasu, H. and Arai, M., *Trans. JSAE*, 21, 5-11 (1980).
[14] Wakuri, Y., Fujii, M., Amitani, T. and Tsuneya, R., *Trans. JSME*, 25, 156, 820-826 (1963).
[15] Zhu, J. and Nishida, K., *20th Symp.(ILASS-Japan) on atomization*, Hiroshima, Japan, December 19-20, 2011.
[16] Zijnen, B.G and Van der Hegge, *Appl.Sci.Res*, Sect. A, 7, 256-276 (1958).